

Robust modeling of quadruply lensed quasars (and random quartets) using Witt's hyperbola

Raymond A. Wynne¹ and Paul L. Schechter^{1,2}

¹MIT Department of Physics, Cambridge, MA 02139

²MIT Kavli Institute for Astrophysics and Space Research, Cambridge, MA 02139

August 21, 2018

We develop a robust method to model quadruply lensed quasars, relying heavily on the work of (Witt, 1996), which showed that for elliptical potentials, the four image positions, the source, and the lensing galaxy lie on a right hyperbola. For the singular isothermal elliptical potential, there exists a complementary ellipse centered on the source which also maps through the four images, with the same axis ratio as the potential but perpendicular to it. We first solve for Witt's hyperbola, reducing the allowable space of models to three dimensions. We then obtain the best fitting complementary ellipse. The simplest models of quadruple lenses require seven parameters to reproduce the observed image configurations, while the four positions give eight constraints. This leaves us one degree of freedom to use as a figure of merit. We applied our model to 29 known lenses, and include their figures of merit. We then modeled 100 random quartets. A selection criterion that sacrifices 20% of the known lenses can exclude 98% of the random quartets.

1 Introduction

Astronomers with experience studying quadruple lenses can reliably determine, by examination of relative positions and fluxes, whether a quartet of point sources is lensed. They have trained a neural network, located between their ears, to identify such systems. With the advent of the Gaia probe, quadruple lenses are being discovered at an astonishing rate (Lemon et al., 2018), and as evidenced

by (Delchambre et al., 2018), there is a clear necessity for robust methods to model these systems.

It is widely thought that the gravitational equipotentials that produce most quadruply lensed quasars can be reasonably approximated by concentric ellipses (Kassiola and Kovner, 1993). The simplest models for isothermal elliptical potentials include seven parameters, and a quartet of image positions gives eight constraints (Keeton, 2001). While that leaves one degree of freedom for use as a figure of merit, it can be difficult to find the best fitting model in that seven dimensional space.

In what follows, we lean heavily on the work of (Witt, 1996), who finds that for elliptical potentials, the positions for all four images, the center of the lens, and the projected (but unobservable) position of the quasar all lie on an hyperbola whose asymptotes align with the potential's major and minor axes. The hyperbola gives us the position angle and restricts the positions of the lens and the source to a one dimensional locus. It reduces the dimensionality of the space to be searched from 7 to 3.

We also show that for the specific case of the singular isothermal elliptical potential, there exists an ellipse mapping through all 4 image positions, whose minor axis is aligned with the major axis of the potential, has an axis ratio inverse to the axis ratio of the potential, and is centered on the source.

We then search along Witt's hyperbola for the source position and axis ratio that minimize the scatter in the lensing strengths determined by the positions of the four quasar images. We use this scatter as our figure of merit.

In Section 2, we briefly explain gravitational lensing,

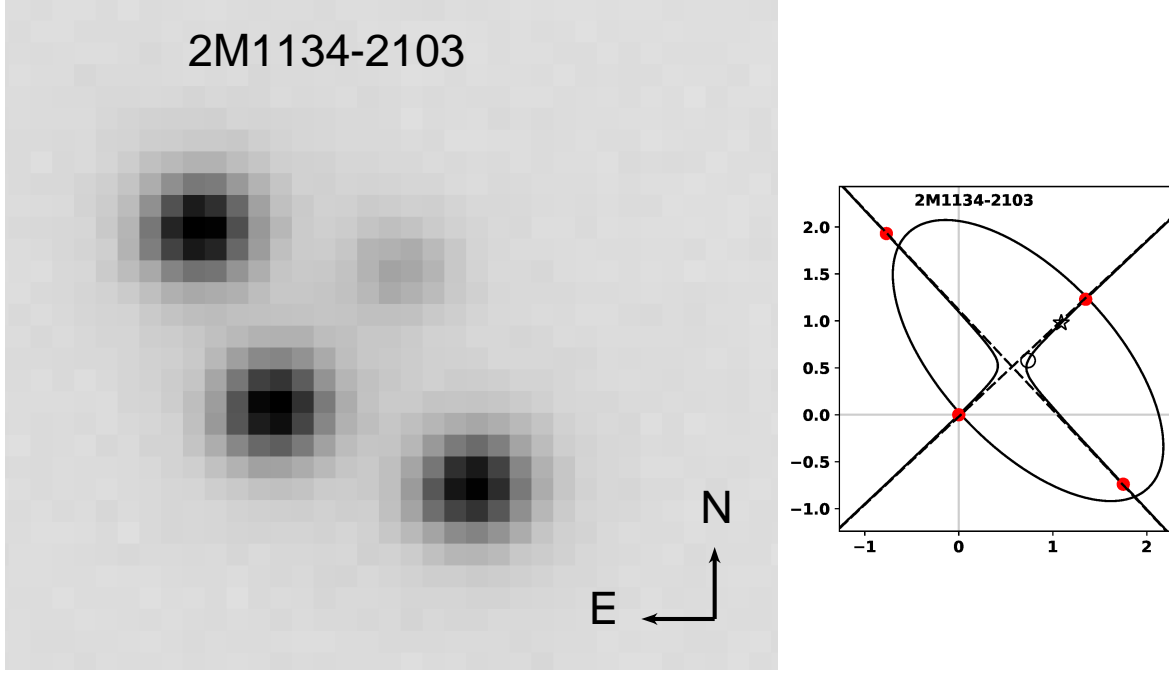


Figure 1: Quadruple lens system 2M1134-2103, with both images at the same scale. On the left is a Sloan *i* filter image taken from the ATLAS survey, and the scale of this figure is $0''.21$ per pixel. On the right is the plot our model produces for 2M1134-2103. The red dots are the image positions, the circle is the source position, and the star is the galaxy position. The parameter values are $b = 0''.92, q = 0.491, \theta = 133.1^\circ$ with $\sigma_{\ln b} = 0.071$.

and discuss the importance of quadruple lenses. In Section 3, we give background into the geometry associated with the quadruple systems, and explain our method of solving for the source position and axis ratio by minimizing the scatter in the lens strength. In Section 4, we compute our proposed figure of merit with a sample of spectroscopically confirmed quadruply lensed quasars. In Section 5, we analyze random quartets, and compare them to the known figures of merit. In Section 6, we discuss the results of the previous sections, and how they might be used to accept or reject the lensing hypothesis.

2 Background

2.1 Gravitational Lensing

Albert Einstein's theory of General Relativity represents gravity as the warping of space-time. Light propagates along paths called geodesics, which are a generalization of the notion of straight lines to curved spaces. When gravitational fields are not strong, one can treat the propagation of light as if there were an index of refraction proportional to the gravitational potential (Narayan and Bartelmann, 1996).

From Fermat's principle, it is known that light follows a path that is stationary in time. For everyday situations, this is the single path that takes the least amount of time for light to travel (Blandford and Narayan, 1986). However, on the astronomical scale, a massive body such as a galaxy can warp space to the degree that multiple paths satisfy this stationary criteria, and multiple images of one source object appear. In this way, the galaxy acts as a lens," although

the French have a better name for the phenomenon: *mirage gravitationnel* (Surdej and Surdej, 2001).

In gravitational lensing, there are three important phenomena and their corresponding equations: time delay, deflection, and distortion. The first deals with the difference in travel time between different paths, the second with the degree to which light gets bent towards the observer, and the final with how the images are magnified and distorted. In this paper, we will only be dealing with deflection, and the associated lens equation,

$$(\vec{u} - \vec{u}_s) = \vec{\nabla}\psi, \quad (1)$$

where \vec{u}_s is the position at which the source would be in the absence of lensing, and ψ is the projected, two-dimensional gravitational potential obtained by integrating the three-dimensional potential along the line of sight. The solutions of the lens equation, \vec{u}_i , give the positions of the images of the source. The $\vec{u} - \vec{u}_s$ term is also known as the deflection, since it is the difference between the observed position and the position the source would have had sans lensing. Therefore, the stronger the gradient in the potential, the greater the deflection (Blandford and Narayan, 1986).

2.2 Quadruple Lenses

Configurations with four images, known as quadruple lenses, are of particular interest. For example, they permit measurements of time delays (Treu and Marshall, 2016), put constraints on cosmological parameters such as the Hubble constant (Suyu et al., 2013), allow study of the structure of quasars (Bate et al., 2008), offer research on

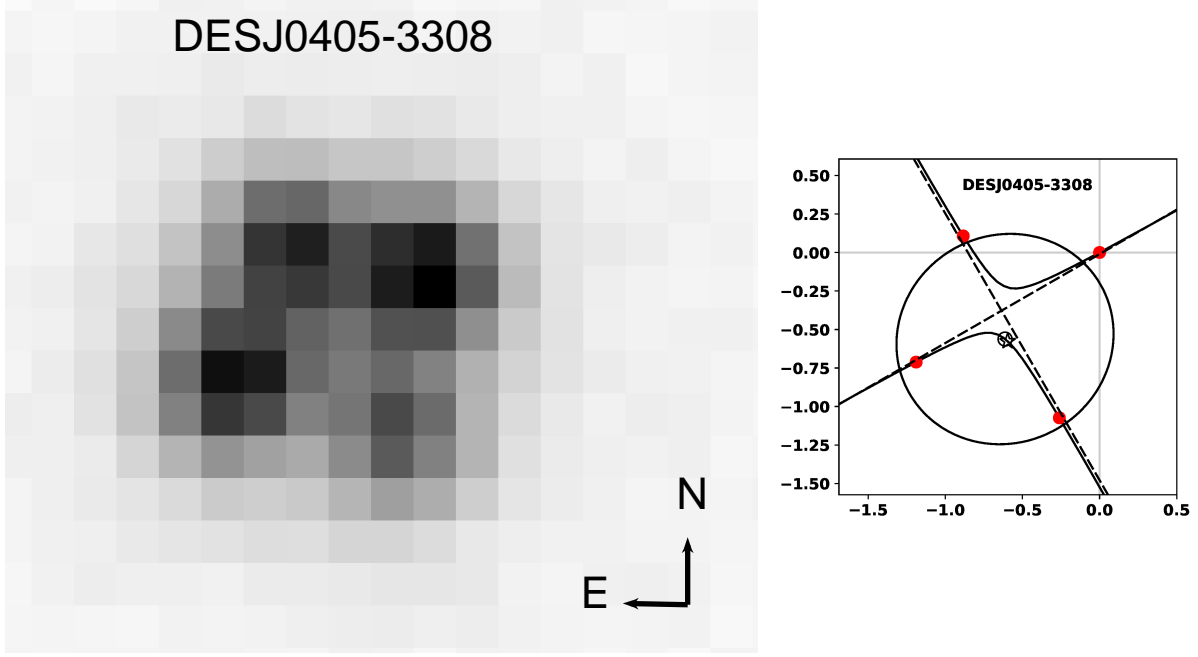


Figure 2: Quadruple lens system DESJ0405-3308, with both images at the same scale. On the left is a Sloan *i* filter image taken from the DES survey, and the scale of this figure is $0''.26$ per pixel. On the right is the plot our model produces for DESJ0405-3308. The red dots are the image positions, the circle is the source position, and the star is the galaxy position. The parameter values are $b = 0''.67$, $q = 0.944$, $\theta = -120.6^\circ$ with $\sigma_{\ln b} = 0.130$.

the stellar content of the lensing galaxy through microlensing (Schechter and Wambsganss, 2004), and can be used as a probe for gas clouds along the line of sight (Zahedy et al., 2017).

Nearly four dozen quadruply lensed quasars have been discovered since PG1115+080 (Weymann et al., 1980), many in recent years. Gaia, whose mission is to create a detailed three-dimensional map of the Milky Way, offers a way to detect these systems (Prusti, 2018); it is expected to discover approximately 2900 quasars, with around 80 having two or more images (Finet and Surdej, 2016).

All of the many applications of quadruply lensed quasars require a model for the gravitational potential. In the gravitational lensing literature, a frequently used model is the elliptical potential. Witt argues that equation (4) applies equally well to a singular isothermal sphere with external shear γ , substituting $1 + \gamma/1 - \gamma$ for $1/q^2$ in equation (4). This is true for the special case in which the shear term in the potential is centered on the source (Witt and Mao, 1997). When the shear term is centered on the galaxy the hyperbola is offset. One way or the other, one might model a singular isothermal sphere with shear following the approach developed below for the singular isothermal elliptical potential.

3 Method

3.1 Witt's Hyperbola

In Witt's paper, he assumes an elliptical potential of the form $\psi = f(r)$, where $r = x^2 + y^2/q^2$ is the equation of an

ellipse with semi-major axis aligned with the x -axis of the coordinate system, and where f is an arbitrary function that describes the variation in spacing of the elliptical equipotentials. For the purposes of this paper, we will use the singular isothermal elliptical potential

$$\psi = b\sqrt{(x - x_g)^2 + (y - y_g)^2/q^2} = bt \quad (2)$$

where b is the lens strength, (x_g, y_g) is the position of the lensing galaxy, $q (< 1)$ is the axis ratio of the potential, and $t = \sqrt{r}$. Note that t plays the role of a distance from the galaxy. The singular isothermal elliptical potential, hereafter SIEP, is a good approximation to the actual potentials produced by the lensing galaxy (Kassiola and Kovner, 1993).

The lens equation for this potential is the following,

$$\vec{u} - \vec{u}_s = \frac{1}{t} \frac{d\psi}{dt} \left[(x - x_g)\hat{x} + \frac{(y - y_g)}{q^2}\hat{y} \right], \quad (3)$$

where (x_s, y_s) is the (unobservable) position of the source. Witt uses only the direction of this equation, taking the ratio of the y component of the displacement vector to the x component of the displacement vector to get

$$\frac{(y - y_s)}{(x - x_s)} = q^{-2} \frac{(y - y_g)}{(x - x_g)} \quad (4)$$

Cross multiplication of (4) gives an equation of the form

$$xy + Ax + By = C, \quad (5)$$

(the coefficients being determined by the galaxy and source positions and the axis ratio), which happens to be a right

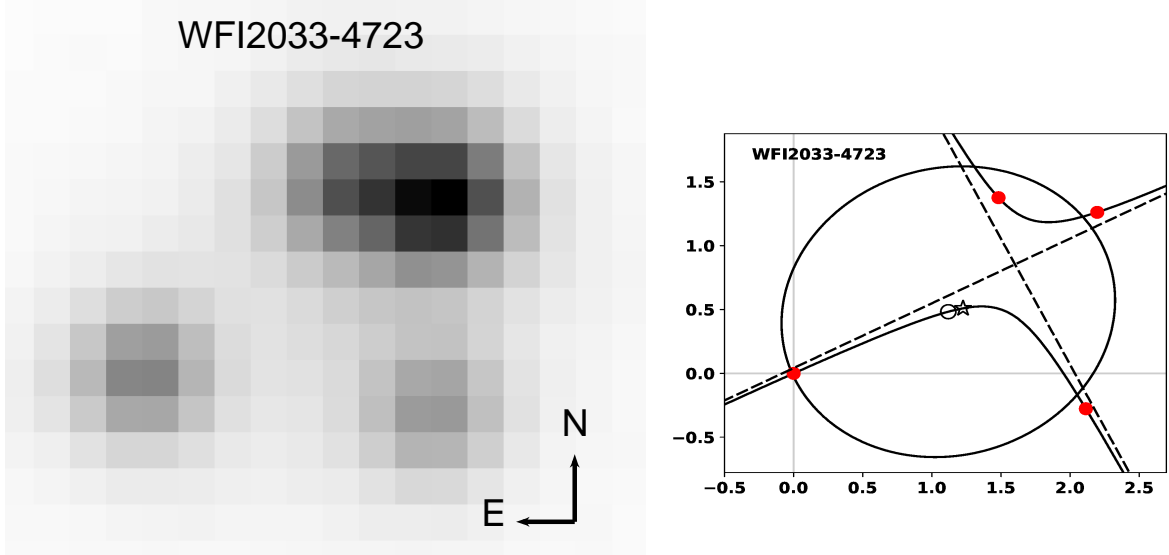


Figure 3: Quadruple lens system WFI2033-4723, with both images at the same scale. On the left is a Sloan *i* filter image taken from the DES survey, and the scale of this figure is $0''.26$ per pixel. On the right is the plot our model produces for WFI2033-4723. The red dots are the image positions, the circle is the source position, and the star is the galaxy position. The parameter values are $b = 1''.12$, $q = 0.906$, $\theta = -63.1^\circ$ with $\sigma_{\ln b} = 0.118$.

hyperbola with asymptotes aligned with the x and y axes. It is clear that, along with the four images, the galaxy and source must lie on this curve, since they satisfy the equation above.

We can with no loss of generality take our coordinate system to be one in which the asymptotes of the hyperbola are not merely aligned with the axes but coincident with them, in which case:

$$xy = W^2, \quad (6)$$

where W is a constant with units of length.

One must apply an arbitrary rotation and translation to Witt's hyperbola to give it the form that it takes in the observed coordinate system. If one shifts the images in the observed system such that one image is at the origin, the equation for the hyperbola takes a simpler form, and is as follows:

$$c_1 x'^2 + c_2 x' y' - c_1 y'^2 + c_3 x' + c_4 y' = 0. \quad (7)$$

We observe only the four images. The position of the source is unknown, the position of the lensing galaxy is often unknown, and even when the position of the lensing galaxy is known, the equipotentials will not have the same shape since the galaxy may not have the same orientation. The image positions are measured in a coordinate system that is rotated and translated by unknown amounts from the coordinate system in which Witt's hyperbola takes its simplest form.

Gravitational lensing requires seven parameters to model a system: the orientation θ , the two galaxy coordinates (x_g, y_g) , the two source coordinates (x_s, y_s) , the lens strength b , and the axis ratio q . Witt's hyperbola has immense power in modeling systems. It not only gives the orientation, but also describes the position of the galaxy

and source by one coordinate, not two. Therefore, Witt's hyperbola reduces the dimensionality of the space to be searched from 7 to 3.

Four observed image positions suffice to determine the four unknown coefficients, $c_1 - c_4$, that uniquely describe the hyperbola. If the lensing potential is *not* elliptical the four images will still give a hyperbola, but we would not expect the source or the galaxy to lie on it. Indeed any four points will produce a right hyperbola, so the hyperbola, by itself, does not tell us if four images are in fact lensed or whether the potential producing them is elliptical.

3.2 A Complementary Ellipse

So far, we have only used the direction of the lens equation. Taking the magnitude squared of each side of (3) and a little algebra gives the equation

$$(x - x_s)^2 + q^2 (y - y_s)^2 = b^2 \quad (8)$$

This equation is important in that for the SIEP, the images appear at the intersection of Witt's hyperbola and an ellipse centered on the unlensed source position, with minor axis aligned with the major axis of the potential.

The four image positions are enough to determine the four parameter values of equation (8). But as in the case of the hyperbola, *any* four points will produce an ellipse once we specify the orientation of the axes. However, unless the images are precisely those of a singular isothermal elliptical potential, the hyperbola determined by equation (7) and the ellipse determined by equation (8) are not consistent with each other. The source position, as determined from the ellipse, will not, in general, lie on the hyperbola.

3.3 Modeling the Singular Isothermal Elliptical Potential

As we wish to construct a self-consistent model, we chose one that is consistent with the hyperbola determined from the four images. We then find an ellipse of the form of equation (8), with the source on our hyperbola, that comes close to passing through the four images.

It is evident from equation (8) that for variable source position and axis ratio, each image will have an associated lens strength b_i . For perfect source position and axis ratio, the b_i will be equal, since the configuration is the result of one lensing strength. Therefore, minimizing the standard deviation of the logarithm of the lens strength,

$$\sigma_{\ln b(x_s, q)} = \sqrt{\langle (\ln b_i - \langle \ln b \rangle)^2 \rangle}, \quad (9)$$

where $\langle \ln b \rangle = \frac{1}{4} \sum_{i=1}^4 \ln b_i$, will give the source position and axis ratio that is in this sense the best fit. In the coincident coordinate system, this is a simple, 2-dimensional minimization problem, since the y-coordinate is given by $\frac{W^2}{x}$. As we show in Appendix A, once the source position and axis ratio are known, the galaxy position is immediately determined. In Appendix B, we show how to determine which branch of the hyperbola the source and galaxy lie on.

Considering the singular isothermal elliptical potential is only a model, albeit a very useful one, the minimum of the scatter will not be at zero. However, this is good; we can use this minimum value as a figure of merit. It can be used to determine how closely a system resembles the singular isothermal elliptical potential, offering insight as to whether a system is a lens or not.

4 Known Lenses

To test our method, we examined 29 known quadruple lenses and recorded their figures of merit. The average value for the figure of merit was $\langle \sigma_{\ln b} \rangle = 0.0531$, and the standard deviation was $\sigma_{\sigma_{\ln b}} = 0.0468$.

We also include three spectroscopically determined quadruply-lensed quasars, and their plots determined by our program. As seen in the plot, the hyperbola goes through all four image positions, along with the source and galaxy positions. In minimizing the scatter, you determine a source position and axis ratio, which in turn determines the ellipse. For the specific case of the singular isothermal elliptical potential, this ellipse will map through the four points; however, since the potential is only a model, this ellipse will not go perfectly through all four images for real systems, but the deviation from the image positions and the ellipse gives a visual for the scatter.

Two systems above caused trouble for our program: HE0230-2130 and PS0630-1201; the former having the largest scatter, and the latter having a galaxy position that lies outside the ellipse. Both of these systems have two lensing galaxies, so their potentials deviate from the ellipti-

| System | Figure of Merit: $\sigma_{\ln b}$ | Axis Ratio |
|----------------|--------------------------------------|------------|
| GRAL1131-4419 | 0.002 | 0.901 |
| SDSSJ1138+0314 | 0.004 | 0.818 |
| ATLAS0259-1635 | 0.009 | 0.892 |
| HE0435-1223 | 0.010 | 0.861 |
| HE1113-06412 | 0.015 | 0.924 |
| PSJ0147+4630 | 0.015 | 0.711 |
| RXJ1131-1231 | 0.016 | 0.746 |
| HS0810+2554 | 0.018 | 0.896 |
| WGD2100-4452 | 0.019 | 0.853 |
| Q2237+030 | 0.020 | 0.876 |
| SDSSJ1251+2935 | 0.027 | 0.769 |
| WGD2038-4008 | 0.033 | 0.771 |
| WFI2026-4536 | 0.036 | 0.765 |
| MG0414+0534* | 0.038 | 0.658 |
| DESJ0408-5354* | 0.041 | 0.818 |
| DESJ0924+0219 | 0.044 | 0.910 |
| RXJ0911+0551* | 0.045 | 0.563 |
| B0712+472 | 0.049 | 0.883 |
| 2M1310-1714 | 0.051 | 0.953 |
| WG0214-2105 | 0.052 | 0.782 |
| PG1115+080 | 0.053 | 0.769 |
| WISE2344-3056 | 0.070 | 0.862 |
| 2M1134-2103 | 0.071 | 0.491 |
| PS0630-1201* | 0.082 | 0.401 |
| SDSSJ1330+1810 | 0.091 | 0.991 |
| WFI2033-4723* | 0.118 | 0.906 |
| H1413+117 | 0.123 | 0.801 |
| DESJ0405-385 | 0.130 | 0.944 |
| HE0230-2130* | 0.220 | 0.707 |

Table 1: List of 29 known quadruples, with their associated figures of merit and axis ratios. * denotes a two-lens system.

cal model more so than systems with one lensing galaxy, which might explain their issues.

There is a natural physical limit $q > 0.5$ to the singular isothermal elliptical potential as an edge-on infinitely flat galaxy with a flat rotation curve produces equipotentials with $q = 0.5$ (Monet, Schechter, and Richstone, 1981). Thus the models for systems with $q \leq 0.5$ are very suspect. The axis ratio $q = 0.49$ derived for 2M1134-2103 argues against our model. (Lucey et al., 2018) find that the system is better modeled as a singular isothermal sphere with external shear $\gamma = 0.34$, among the highest known for quadruply lensed quasars.

As Witt mentioned, there is ambiguity in determining the orientation of the system. The correct orientation has the asymptotes of the hyperbola aligned with the axes, but there are two unique orientations with that property. In Appendix C, we sort out this issue.

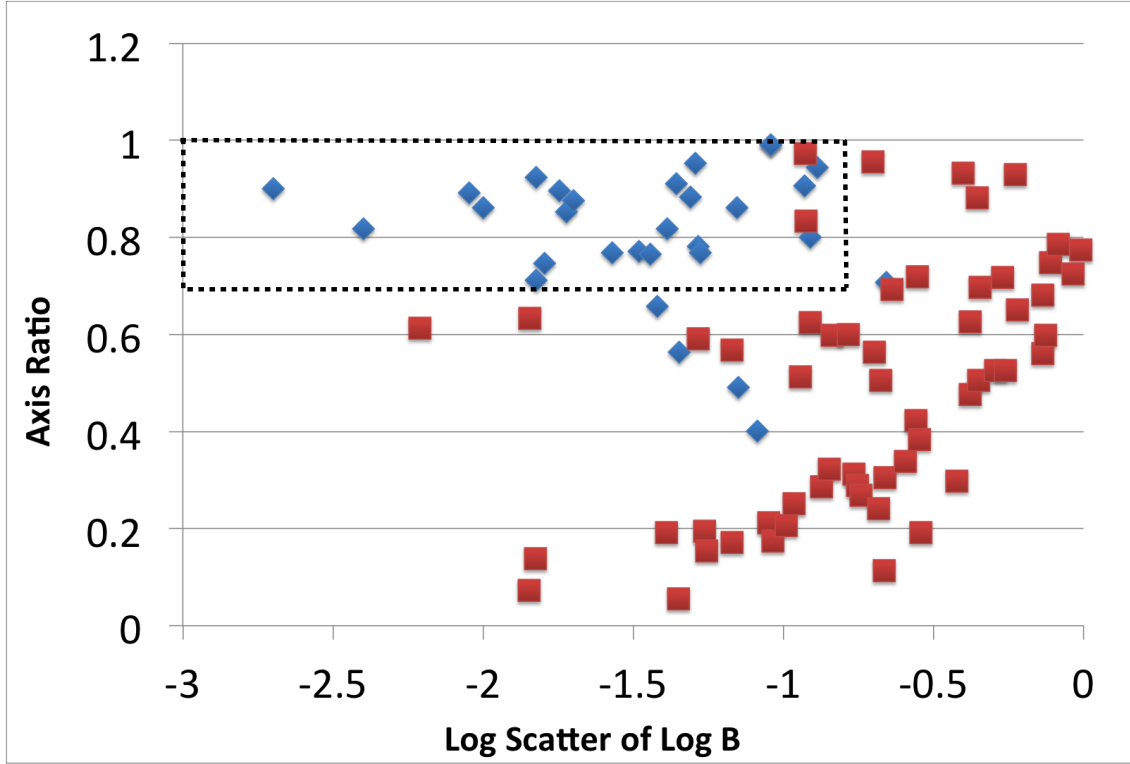


Figure 4: Scatter plot of the logarithm of the figure of merit vs the axis ratio. Twenty-nine known lenses are in blue, and fifty-six random quartets are in red. The dashed box catches 24 of the 29 known lenses, as well as 2 of the random quartets.

5 Random Quartets

To see how well our figure of merit discriminated between genuine lenses and random quartets, we generated 100 random quartets within the unit circle and applied our program to them. We rejected the cases that had three or more images on one branch of the hyperbola.

In Figure 4, we plot the logarithm of the scatter versus the axis ratio for our known system and random quartets that passed our criteria above. We hoped for more separation between the real and random quartets, but every model has its downsides. The dashed box catches 24 of the 29 known lenses, as well as 2 of the 100 random quartets. So roughly, our model has a 2% false positive rate. Two percent of 80,000, which is roughly the number of quartets identified by (Delchambre et al., 2018), is 1,600; in other words, a lot of eyeballing is still required.

The systems that lie below the box include RXJ0911+0551 and 2M1134-2103 for which external shear rather than the ellipticity of the lens is thought to dominate the quadrupole term in the potential. MG0414+0534 and PS0630-1201, also below the box, are systems for which a second lensing galaxy contributes significantly to the potential. HE0230-2130, another double lens, lies to the right of the box. While it's a shame to lose these systems, they are all pretty different from our adopted model.

It is clear from the comparison of our lensed systems and

our random quartets that positions alone do not permit perfect discrimination between the two. If this discrimination does not suffice for some particular task, there is additional information that might be brought to bear on improving it – the relative fluxes of the four images.

In the absence of micro-lensing, the relative fluxes that our model parameters predict for the four images can be obtained from the distortion equation. These cannot be used directly, because micro-lensing is expected to be universal in quadruply lensed quasars (Witt, Mao, and Schechter, 1995). (Yahalom, Schechter, and Wambsganss, 2017) have shown how one might take micro-lensing into account in assessing the likelihood that observed flux ratios are consistent with the lens model and microlensing. One would then still need to decide how to combine the present astrometric discrimination and the photometric figure of merit.

6 Conclusion

We discussed the basics of gravitational lensing, and the phenomenon of quadruple lenses. We then developed a method for modeling quadruply lensed quasars through the use of Witt's hyperbola and the complementary ellipse, as well as assigning a figure of merit to potential systems. We applied this method to 29 known quadruply lensed systems and 100 random quartets, and included their figures of merit. For future systems, this figure of merit can help

astronomers determine if a newly discovered system is the product of gravitational lensing, or merely a random configuration.

Acknowledgements: We thank Professor Alar Toomre for asking how we could tell quadruply lensed quasars from random quartets. We thank Professor Chuck Keeton of Rutgers for setting us straight about ellipses early in this effort and his pointing us toward Witt's work. Finally, we thank the MIT Undergraduate Research Opportunities Program for support.

References

- Bate, N. F. et al. (2008). "A microlensing study of the accretion disc in the quasar MG 0414+0534". In: *MNRAS* 391, pp. 1955–1960.
- Blandford, R. and R. Narayan (1986). "Fermat's principle, caustics, and the classification of gravitational lens images". In: *The Astrophysics Journal* 310, pp. 568–582.
- Delchambre, L. et al. (2018). "Gaia GraL III - Gaia DR2 Gravitational Lens Systems: A systematic blind search for new lensed systems". In: *ArXiv e-prints*. "arXiv": 1807.02845.
- Finet, F. and J. Surdej (2016). "Multiply imaged quasi-stellar objects in the Gaia survey". In: *A&A* 590, A42.
- Kassiola, A. and I. Kovner (1993). "Elliptic Mass Distributions versus Elliptic Potentials in Gravitational Lenses". In: *ApJ* 417, p. 450.
- Keeton, C. R. (2001). "A Catalog of Mass Models for Gravitational Lensing". In: *ArXiv Astrophysics e-prints*. eprint: astro-ph/0102341.
- Lemon, C. A. et al. (2018). "Gravitationally Lensed Quasars in Gaia: II. Discovery of 24 Lensed Quasars". In: *MNRAS* 479, pp. 5060–5074.
- Lucey, J. R. et al. (2018). "Serendipitous discovery of quadruply imaged quasars: two diamonds". In: *MNRAS* 476, pp. 927–932.
- Monet, D. G., P. L. Schechter, and D. O. Richstone (1981). "The effect of massive disks on bulge isophotes". In: *ApJ* 245, pp. 454–458.
- Narayan, R. and M. Bartelmann (1996). "Lectures on Gravitational Lensing". In: *ArXiv Astrophysics e-prints*. eprint: astro-ph/9606001.
- Prusti, T. (2018). "The Gaia mission status". In: *IAU Symposium*. Ed. by A. Recio-Blanco et al. Vol. 330. IAU Symposium, pp. 7–12.
- Schechter, P. L. and J. Wambsganss (2004). "The dark matter content of lensing galaxies at 1.5 R_e". In: *Dark Matter in Galaxies*. Ed. by S. Ryder et al. Vol. 220. IAU Symposium, p. 103.
- Surdej, J. and A. Surdej (2001). "Les mirages gravitationnels-IV". In: *Le Ciel* 63, pp. 21–26.
- Suyu, S. H. et al. (2013). "Two Accurate Time-delay Distances from Strong Lensing: Implications for Cosmology". In: *ApJ* 766, p. 70.
- Treu, T. and P. J. Marshall (2016). "Time delay cosmography". In: *A&A Rev.* 24, p. 11.

- Weymann, R. J. et al. (1980). "The triple QSO PG1115+08 - Another probable gravitational lens". In: *Nature* 285, pp. 641–643.
- Witt, H. J. (1996). "Using Quadruple Lenses to Probe the Structure of the Lensing Galaxy". In: *ApJ* 472, p. L1.
- Witt, H. J. and S. Mao (1997). "Probing the structure of lensing galaxies with quadruple lenses: the effect of 'external' shear". In: *MNRAS* 291, pp. 211–218.
- Witt, H. J., S. Mao, and P. L. Schechter (1995). "On the universality of microlensing in quadruple gravitational lenses". In: *ApJ* 443, pp. 18–28.
- Yahalom, D. A., P. L. Schechter, and J. Wambsganss (2017). "A Quadruply Lensed SN Ia: Gaining a Time-Delay...Losing a Standard Candle". In: *ArXiv e-prints*. "arXiv": 1711.07919.
- Zahedy, F. S. et al. (2017). "On the radial profile of gas-phase Fe/ α ratio around distant galaxies". In: *MNRAS* 466, pp. 1071–1081.

Appendix A

In this appendix, we show how to determine the galaxy position from the source position and axis ratio. Using the direction of the lens equation, Witt derived equation (4). This equation gives us a right hyperbola mapping through the four images, the source, and the galaxy positions. Essentially, this hyperbola gives us the possible locations for image positions given the configuration of the system. For simplification, moving the y-terms to the left and x-terms to the right, one recovers

$$\frac{(y - y_s)}{(y - y_g)} = q^{-2} \frac{(x - x_s)}{(x - x_g)} \quad (10)$$

In the coincident coordinate system, the y-coordinate is given by W^2/x , so as x goes to zero, the left hand side approaches unity while the right hand side approaches $q^{-2} \frac{x_s}{x_g}$. Therefore, for perfect source position and axis ratio, the x-coordinate of the galaxy position is given by

$$x_g = \frac{x_s}{q^2}, \quad (11)$$

and since the galaxy also lies on the hyperbola, the y-coordinate is immediately determined.

Appendix B

In the coincident coordinate system, the branches of the hyperbola are separated by the x and y axes. The question arises as to which branch the galaxy and source will lie on. To determine this, we minimize the scatter, subject to the constraint that the source lies within the image configuration, on both branches of the hyperbola. The branch that the source which minimizes the scatter lies on is determined to be the correct branch.

Appendix C

The hyperbola gives us two unique orientations for the system. However, the ellipse determines which of these systems is correct. Looking at equation (8), it is easy to see that coefficient for y^2 is simply q^2 . Thus, determining the equation for the ellipse using the four image positions determines the axis ratio. Therefore, if $q > 1$, you know you are in the wrong orientation. If you happen to be in the orientation where $q > 1$, rotating by $\frac{\pi}{2}$ gets you into the

correct orientation.

However, since the ellipse determined by the image positions is only accurate for near-perfect systems, it might not give the orientation which minimizes scatter. Therefore, we use our method for four possible orientations: observed, rotated by $\pm \frac{\pi}{2}$, and rotated by π . The orientation which gives the smallest scatter is determined to be the correct orientation. We then rotate the found source and galaxy positions back into the observed frame, if need be.